DLES 13

13th ERCOFTAC Workshop on Direct & Large Eddy Simulation

26-28 October 2022

Udine, Italy

UNIVERSITÀ DEGLI STUDI DI UDINE

ERCOFTAC

European Research Community On Flow, Turbulence And Combustion

WORKSHOP
Direct and Large-Eddy Simulation 13
October 26th-29th 2022, Udine, Italy

MACHINE LEARNING MODELS FOR SUBGRID SCALE TENSORS OF 2D RAYLEIGH-BÉNARD CONVECTION

L. Biferale[1], M. Buzzicotti[1], P. Cifani[2,3], B.J. Geurts[2,4], J-M. Leahy[2,5]
[1] Dept. of Physics and INFN, University of Rome "Tor Vergata," Rome, IT [2] Dept. of Applied Mathematics, University of Twente, Enschede, NL [3] Gran Sasso Science Institute, L'Aquila, IT [4] Dept. of Applied Physics, Eindhoven University of Technology, Eindhoven, NL [5] Dept. of Mathematics, Imperial College London, London, UK

RAYLEIGH-BÉNARD CONVECTION (RBC)

We consider Rayleigh-Bénard convection (RBC) in two-dimensions using the Oberbeck-Boussinesq approximation of the Navier-Stokes equations with constant kinematic viscosity $\nu > 0$, thermal diffusivity $\kappa > 0$, coefficient of thermal expansion α, gravitational magnitude g in the negative $\hat{\mathbf{z}}$-direction, periodic boundary conditions in the horizontal direction with length L, no-slip boundary conditions in the vertical direction with length H, and isothermal temperature T_{top} at the top and T_{bot} at the bottom. The system models a buoyancy-driven flow in a fluid layer heated from below and cooled from above. Denoting the aspect ratio of the domain by $\Lambda := L/H$, the equations governing the nondimensionalized velocity $\mathbf{u}$, temperature T, and pressure p are

$$\begin{cases} \partial_t \mathbf{u} + \nabla\cdot(\mathbf{u}\otimes\mathbf{u}) - \nabla p = \sqrt{\frac{\mathrm{Pr}}{\mathrm{Ra}}}\Delta\mathbf{u} + T\hat{\mathbf{z}}\,, \\ \partial_t T + \nabla\cdot(\mathbf{u}T) = \frac{1}{\sqrt{\mathrm{Pr}\,\mathrm{Ra}}}\Delta T\,, \\ \nabla\cdot\mathbf{u} = 0\,, \end{cases} \tag{1}$$

where the Rayeligh and Prandtl numbers are denoted $\mathrm{Ra} := \frac{\alpha\Delta T g H^2}{\nu\kappa}$ and $\mathrm{Pr} := \frac{\nu}{\kappa}$. The boundary conditions are:

$$\begin{cases} \mathbf{u}(t,x,z) = \mathbf{0} & (t,x,z) \in \mathbb{R}_+ \times [0,\Lambda] \times \{0,1\}\,, \\ T(t,x,z) = 1 & (t,x,z) \in \mathbb{R}_+ \times [0,\Lambda] \times \{0\}\,, \\ T(t,x,z) = 0 & (t,x,z) \in \mathbb{R}_+ \times [0,\Lambda] \times \{1\}\,, \end{cases}$$

and $\mathbf{u}, T, p$ are periodic with period Λ in the x-variable. The RBC initial-value problem is well-posed in the standard L^2-Sobolev classes with phase space denoted X, and the solution semigroup $\{S_t\}_{t\geq 0} : X \to X$ has a compact connected finite-dimensional maximal attractor $\mathcal{A} \subset X$ [1]. While the existence of an inertial manifold (i.e., $\exists$ a finite dimensional restriction) is unknown, it has recently been shown that there exists a finite-dimensional determining form involving only the velocity field [2]. The LES and a priori learning problem that we describe below can be understood as a learning problem for an approximate inertial map, with the filter replacing the 'slow' dissipation operator eigenspace.

A key diagnostic of RBC is the Nusselt number Nu, which is defined to be the ratio of bulk-averaged vertical heat flux Q from both conduction and convection to flux $\kappa\Delta T/H$ from conduction alone. In terms of nondimesional quantities,

$$\mathrm{Nu} := \langle(\sqrt{\mathrm{Pr}\,\mathrm{Ra}}\;\mathbf{u}T - \nabla T)\cdot\hat{\mathbf{z}}\rangle = 1 + \sqrt{\mathrm{Pr}\,\mathrm{Ra}}\langle u_z T\rangle\,,$$

where $\langle\cdot\rangle$ denotes the time and spatial average operator and $u_z = \mathbf{u}\cdot\hat{\mathbf{z}}$ denotes the vertical component of the velocity. The asymptotic behavior of Nu as $\mathrm{Ra}\to\infty$ is a long standing open problem [3]. Experiments and analysis have yet to confirm the 'classical' scaling $\mathrm{Nu}\sim\mathrm{Ra}^{1/3}$ or 'ultimate' scaling $\mathrm{Ra}^{1/2}$, which has been proved to be the upper limit [4]

SUBGRID-SCALE (SGS) TENSORS

We define a filtering operator acting on fields defined on the spatial domain via a product Gaussian filter with constant horizontal width Δ_x and non-uniform vertical width $\Delta_y(y)$ that is smaller near the vertical boundary. Applying the filter to (1) and using the notation $\overline{\cdot}$ for filtered fields, we find

$$\begin{cases} \partial_t \overline{\mathbf{u}} + \nabla\cdot(\overline{\mathbf{u}}\otimes\overline{\mathbf{u}}) - \nabla\overline{p} = \sqrt{\frac{\mathrm{Pr}}{\mathrm{Ra}}}\Delta\overline{\mathbf{u}} + \overline{T}\hat{\mathbf{z}} - \nabla\cdot\boldsymbol{\tau} + \mathbf{e}_{\mathbf{u}}\,, \\ \partial_t\overline{T} + \nabla\cdot(\overline{\mathbf{u}}\overline{T}) = \frac{1}{\sqrt{\mathrm{Pr}\,\mathrm{Ra}}}\Delta\overline{T} - \nabla\cdot\mathbf{q} + \mathbf{e}_T\,, \\ \nabla\cdot\overline{\mathbf{u}} = 0\,, \end{cases} \tag{2}$$

where the SGS stress and heat flux tensors are denoted

$$\boldsymbol{\tau} = \tau(\mathbf{u}) = \overline{\mathbf{u}\otimes\mathbf{u}} - \overline{\mathbf{u}}\otimes\overline{\mathbf{u}} \quad \text{and} \quad \mathbf{q} = \mathbf{q}(\mathbf{u},T) = \overline{\mathbf{u}T} - \overline{\mathbf{u}}\overline{T}\,,$$

and the fields $\mathbf{e}_{\mathbf{u}}, \mathbf{e}_T$ are errors that arise due to non-uniformity. We define the total SGS by $\boldsymbol{\mathcal{T}} : X\times[0,\Lambda]\times[0,1]\to\mathbb{R}^6$ by $\boldsymbol{\mathcal{T}}(\mathbf{u},T) = [\boldsymbol{\tau}(\mathbf{u}), \mathbf{q}(\mathbf{u},T)]^\top$. It follows that

$$\mathrm{Nu} = 1 + \sqrt{\mathrm{Pr}\,\mathrm{Ra}}\,\langle\overline{u_z}\overline{T} + q_z\rangle + e_{\mathrm{Nu}}\,, \tag{3}$$

where $e_{\mathrm{Nu}} = \langle u_z T - \overline{u_z T}\rangle$ is the commutator error.

CONTINUUM A PRIORI LEARNING

Denote by $F_\theta : [0,\Lambda]\times[0,1]\times\mathbb{R}^2\times\mathbb{R}\times\mathbb{R}^{2\times 2}\times\mathbb{R}^2\to\mathbb{R}^6$, $\theta\in\mathbb{R}^{d_\theta}$, a fully connected five hidden-layer neural network (NN) with tanh activation functions and hidden layer depth 512. The NN induces an SGS $\boldsymbol{\mathcal{T}}_\theta : X\times[0,\Lambda]\times[0,1]\to\mathbb{R}^6$:

$$\boldsymbol{\mathcal{T}}_\theta(\mathbf{u},T)(x,z) = F_\theta(x,z,\mathbf{u}(x,z),T(x,z),\nabla\mathbf{u}(x,z),\nabla T(x,z))\,,$$

with components denoted $[\tau_\theta, \mathbf{q}_\theta]^\top := \boldsymbol{\mathcal{T}}_\theta(\mathbf{u},T)$.[1] The parametric family $\{\boldsymbol{\mathcal{T}}_\theta\}_{\theta\in\mathbb{R}^{d_\theta}}$ induces a closure model

$$\begin{cases} \partial_t\overline{\mathbf{u}}_\theta + \nabla\cdot(\overline{\mathbf{u}}_\theta\otimes\overline{\mathbf{u}}_\theta) - \nabla\overline{p}_\theta = \sqrt{\frac{\mathrm{Pr}}{\mathrm{Ra}}}\Delta\overline{\mathbf{u}}_\theta + \overline{T}_\theta\hat{\mathbf{z}} - \nabla\cdot\boldsymbol{\tau}_\theta(\overline{\mathbf{u}}_\theta,\overline{\mathbf{q}}_\theta)\,, \\ \partial_t\overline{T}_\theta + \nabla\cdot(\overline{\mathbf{u}}_\theta\overline{T}_\theta) = \frac{1}{\sqrt{\mathrm{Pr}\,\mathrm{Ra}}}\Delta\overline{T}_\theta - \nabla\cdot\mathbf{q}_\theta(\overline{\mathbf{u}}_\theta,\overline{T}_\theta)\,, \\ \nabla\cdot\overline{\mathbf{u}}_\theta = 0\,. \end{cases} \tag{4}$$

[1] It suffices to define a parametrization of, e.g., the upper triangular part of $\overline{\mathbf{u}\otimes\mathbf{u}} - \overline{\mathbf{u}}\otimes\overline{\mathbf{u}}$ and take the range of F_θ to be $\mathbb{R}^5$, but we avoid this in the presentation for simplicity.

We assume (4) is well-posed and induces a solution semigroup $\{\bar{S}_{\theta,t}\}_{t\geq 0} : X \to X$ with global attractor $\overline{\mathcal{A}}_\theta$. We would like to choose $\theta^* \in \mathbb{R}^{d_\theta}$ such that the closure dynamics $\{\overline{S}_{\theta,t}\}$ approximates the filtered true dynamics $\{\overline{S_t}\}$. Perhaps more modestly, we would like their first and second order statistics to agree approximately, and in particular (see Figure 1),

$$\mathrm{Nu} \approx \mathrm{Nu}_{\theta^*} := 1 + \sqrt{\mathrm{Pr}\,\mathrm{Ra}}\,\langle \overline{u}_{\theta^*,z}\overline{T}_{\theta^*} + q_{\theta^*,z}\rangle. \qquad (5)$$

Letting $\mu \in \mathcal{P}(X)$ denote an ergodic invariant measure of $\{S_t\}$, we define the a priori generalization error by

$$\begin{aligned} L(\theta) &= \frac{1}{2}\int_X |\boldsymbol{\mathcal{T}}(\mathbf{u},T) - \boldsymbol{\mathcal{T}}_\theta(\overline{\mathbf{u}},\overline{T})|^2_{L^2}\,d\mu(\mathbf{u},T) \\ &= \frac{1}{2}\lim_{T'\to\infty}\frac{1}{T'}\int_0^{T'} |\boldsymbol{\mathcal{T}}(\mathbf{u}_t,T_t) - \boldsymbol{\mathcal{T}}_\theta\left(\overline{\mathbf{u}_t},\overline{T_t}\right)|^2_{L^2}\,dt\,, \end{aligned}$$

and aim to find $\theta^* \in \arg\min_{\theta\in\mathbb{R}^{d_\theta}} L(\theta)$. The convenient property of the a priori loss is that it translates to a supervised learning problem. Indeed, one creates the data set

$$\mathcal{D} := \{(X_t := (\overline{u}_{t+T_0}, \overline{T}_{t+T_0}),\ \ Y_t := \boldsymbol{\mathcal{T}}(u_{t+T_0}, T_{t+T_0})\}_{t\leq T'}$$

for a burn-in time T_0 and total length T', and then minimizes

$$\hat{L}(\theta) = \frac{1}{2}\frac{1}{T'}\int_0^{T'} |Y_t - \boldsymbol{\mathcal{T}}_\theta(X_t)|^2_{L^2}\,dt\,.$$

Recent work on invariant measures of Itô diffusions in finite-dimensions [5], suggests that the error between the one and two point statistics of $\{\overline{S_t}\}$ and $\{\overline{S}_{\theta,t}\}$ can be bound in terms of the a priori generalization error, with a bias term depending on the non-uniformity 'errors' $\mathbf{e_u}, e_T$ in (2). There is additional error in the computation of unfiltered semigroup $\{S_t\}$ statistics. However, for the Nusselt number, the parameteric SGS heat flux $\mathbf{q}_\theta$ can be used in the recovery of Nu, with the only additional error being due to $\mathbf{e}_{\mathrm{Nu}}$ (cf. (3) and (5)). The non-uniformity errors, which we observe to be small in our numerical experiments, serve as placeholders for the, potentially, larger errors that appear in the discrete a priori learning problem due to the discrepancy between the discretization errors between fine and coarse grid (cf. (2) and (6)).

DISCRETE A PRIORI LEARNING

In our simulations, we set $\mathrm{Pr} = 1$ and $\Lambda = 2$ and investigate $\mathrm{Ra} \in \{10^k\}_{k=8}^{13}$. We integrate (1) in time using an explicit low-storage third-order Runge-Kutta scheme and in space using an energy-conserving second-order finite difference method on a staggered grid. The CFL condition determines the time step size δt as a function of Ra and the spatial step sizes $\delta x = 2^{-n}$ and δz. Since resolving the boundary layer improves the fidelity of the simulations, we use a non-uniform grid in the wall-normal direction with the $n_z = 2^n + 1$ grid points distributed according to a tanh profile, and the level of refinement chosen according to the Prandtl-Blasius (PB) theory developed in [7]. A hybrid MPI-openMP decomposition is used for parallelisation. We refer to [6] for more details.

We define a filtering operation on the 'fine' spatial-grid, denoted by G_δ, using a numerical implementation of the non-uniform product Gaussian filter described above. The total discrete filtering operation is the composition of the Gaussian filter with a 'projection' onto the coarse gird, denoted by G_Δ, with horizontal step size $\Delta x = 2^c\delta x$ and number of vertical grid points $N_z = 2^{-c}n_z$. The coarse time step size $\Delta t = M\delta t$, $M \in \mathbb{N}$, is chosen according to the CFL condition.

Denote by $\Phi_\delta : X_\delta \to X_\delta$ and $\Phi_\Delta : X_\Delta \to X_\Delta$ the fine grid and uncorrected coarse grid one-step solution maps, respectively. The fine grid solution $\mathbf{x}^\delta : \mathbb{N} \to X_\delta$ satisfies $\mathbf{x}^\delta_{n+1} = \Phi_\delta(\mathbf{x}^\delta_n)$. Noting that the M-times composition Φ_δ^M and Φ_Δ have comparable time scales, we find

$$\overline{\mathbf{x}^\delta_{n+M}} = \Phi_\Delta\left(\overline{\mathbf{x}^\delta_n}\right) + \nabla^\Delta\cdot\boldsymbol{\mathcal{T}}\left(\mathbf{x}^\delta_n\right) + \mathbf{e}^{\delta,\Delta}_n\,, \qquad (6)$$

where $\nabla^\Delta\cdot$ denotes the coarse grid divergence operator and $\mathbf{e}^{\delta,\Delta}$ arises due to the i) non-uniformity of the filter and ii) discrepancy between the fine and coarse time and space-grid discrete differential operators. The parametric coarse grid one-step solution map $\Phi_{\theta,\Delta} : X_\Delta \to X_\Delta$ is defined using $\boldsymbol{\mathcal{T}}_\theta$, so that the coarse grid solution $\overline{\mathbf{x}}^\Delta_\theta : \mathbb{N} \to X_\Delta$ satisfies

$$\overline{\mathbf{x}}^\Delta_{\theta,m+1} = \Phi_{\theta,\Delta}(\overline{\mathbf{x}}^\Delta_{\theta,m+1}) := \Phi_\Delta(\overline{\mathbf{x}}^\Delta_{\theta,m+1}) + \nabla^\Delta\cdot\boldsymbol{\mathcal{T}}_\theta(\overline{\mathbf{x}}^\Delta_{\theta,m+1})\,.$$

We then define the supervised learning problem as above.

NUMERICAL EXPERIMENTS

We will perform a priori and a posteriori tests of the NN closure model and compare it with the null, Clark, inverse-filtering, and dynamic Smagorinsky SGS models. Furthermore, we will investigate whether the NN SGS model can extrapolate to different Ra and c. In Figure 1, we provide an a posteriori test of Nu for $c = 4$ at $\mathrm{Ra} = 10^{12}$. This result shows favorable comparison of the NN closure with DNS reference computed on the fine grid with $2^{13} \times 2^{12}$ points.

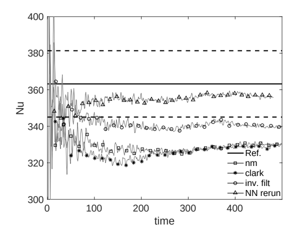

Figure 1: Running time average of Nu for $c = 4$ at $\mathrm{Ra} = 10^{12}$.

Acknowledgments. This research has received funding from the European Research Council (ERC) under the European Union's Horizon 2020 research and innovation programme (grant agreement No 882340).

REFERENCES

[1] Foias, C., Manley, O. and Temam, R. Attractors for the Bénard problem: existence and physical bounds on their fractal dimension. Nonlinear Anal. Theory Methods Appl.. **11**, 939-967 (1987)
[2] Cao, Y., Jolly, M. and Titi, E. A Determining Form for the 2D Rayleigh-Bénard Problem. ArXiv Preprint 1907.00387. (2019)
[3] Charles R. Doering Turning up the heat in turbulent thermal convection. PNAS. **117**, 9671-9673 (2020)
[4] Otto, F., Pottel, S. amd Nobili, C. Rigorous Bounds on Scaling Laws in Fluid Dynamics. Mathematical Thermodynamics Of Complex Fluids: Cetraro, Italy 2015. pp. 101-145 (2017)
[5] Zhang, H., Harlim, J. and Li, X. Error bounds of the invariant statistics in machine learning of ergodic Itô diffusions. Phys. D: Nonlinear Phenom.. **427** pp. 133022 (2021)
[6] Hasslberger, J., Cifani, P., Chakraborty, N. and Klein, M. A direct numerical simulation analysis of coherent structures in bubble-laden channel flows. J. Fluid Mech.. **905** pp. A37 (2020)
[7] Shishkina, O., Stevens, R., Grossmann, S. and Lohse, D. Boundary layer structure in turbulent thermal convection and its consequences for the required numerical resolution. New J. Phys.. **12**, 075022 (2010)